Journal of
Ceramic Science
and Technology

J. Ceram. Sci. Technol., **12** [2] 63-70 (2021)
DOI: 10.4416/JCST2021-00002
available online at: http://www.ceramic-science.com

Review

Optimization of the Heat Treatment Process for Preparing Light-Green Glass-Ceramics from Blast Furnace Slag

Yi-ci Wang[1], Rui-xin Wang[*1], Yi-fan Wang[1], Jia Liu[1], Yi-fan Chai[1], Guo-ping Luo[1]

[1]School of Materials and Metallurgy, Inner Mongolia University of Science and Technology, Inner Mongolia, Baotou, 014010, China

received February 15, 2021; received in revised form April 12, 2021; accepted April 15, 2021

Abstract

Light-green slag-based glass-ceramics were prepared using blast furnace water-quenched slag from the Baotou Iron and Steel Group as the main raw material. An orthogonal experimental design was used to study the influence of heat treatment process parameters on the flexural strength, devitrified mineral composition, and microstructure of the glass-ceramics. The order of influencing factors is crystallization temperature > nucleation time > nucleation temperature > crystallization time. The optimal heat treatment protocol comprised a nucleation temperature of 660 °C, a nucleation time of 2.5 h, a crystallization temperature of 822 °C, and a crystallization time of 2 h. The mineral composition and microstructure of the glass-ceramics were analyzed by means of X-ray diffraction (XRD), scanning electron microscopy (SEM), and energy-dispersive spectroscopy (EDS). The main crystal phase of all glass-ceramics prepared under the different heat treatment regimes was fluorapatite, $Ca_5(PO_4)F_3$. Under optimal heat treatment, the number of crystal grains of the glass-ceramic was large, their distribution was uniform and dense, the degree of crystallinity was high, and the flexural strength was 76.83 MPa.

Keywords: Blast furnace slag, light-green glass-ceramic, orthogonal design; heat treatment, microstructure

I. Introduction

Following the 19th National Congress of the Communist Party of China in 2017, the Inner Mongolia Autonomous Region issued an implementation plan for the development of high-quality emerging industries in this region. This plan encourages the use of fly ash, coal gangue, slag, and other bulk industrial solid wastes to produce new materials and thereby support Baotou in building a national "urban mineral" demonstration base.

Glass-ceramics are basic glasses with specific compositions that are subjected to controlled nucleation and crystallization heat treatment processes to precipitate crystals from an amorphous glass body, thereby preparing a composite material in which glass and microcrystalline phases coexist [1 – 23]. Blast furnace slag was the first raw material used to develop slag glass-ceramics and has a history spanning more than 30 years [4]. The use of these slags to prepare glass-ceramics is an effective way to improve utilization and value of these industrial wastes as well as to reduce environmental pollution. It has become a research topic attracting considerable interest in recent years.

In 1965, Kemantaski [5] used blast furnace slag to make glass-ceramics, which were named slagceram. Agarwal and Speyer [6] developed wear-resistant microcrystalline ceramic products using CaO-rich blast furnace slag, which had twice the wear resistance of basic glass. Khater [7] used Egyptian steel slag to successfully produce glass-ceramics, reporting a utilization of 57 %. Francis [8] used blast furnace slag and dust to prepare magnetic glass-ceramics. Fan, C.S. and Li, K.C. [9] employed waste glass from thin-film transistor liquid-crystal displays (TFT-LCD) and slag from a basic oxygen furnace (BOF) to produce CaO-MgO-Al_2O_3-SiO_2 (CMAS) glass-ceramics by means of vitrification and further heat treatment of compacts of the obtained glass powders for densification and crystallization. Zhang *et al.* [10] used blast furnace slag produced by the Kunming Iron and Steel corporation in Yunan province as raw materials together with mineral materials such as quartz, feldspar, fluorite, dolomite, calcite and other chemical reagents such as sodium hexametaphosphate and Cr_2O_3, to prepare glass-ceramics with the melting method. The major crystalline phase in the glass-ceramics was wollastonite ($CaSiO_3$) and diopside ($Ca{\cdot}Mg(SiO_3)_2$), the granules of which are thin small, closely and evenly distributed. Zhao *et al.* [11] used a low-cost technology to prepare glass-ceramics based on direct heat treatment with molten glass containing blast furnace slag and silica sand. Thanks to the utilization of the heat from the molten slag, the energy cost was much lower than that with the conventional method. The utilized ratio of slag was about 90 % and the optimum heat treatment schedule for glass-ceramics was confirmed with an $L_9(3^4)$ orthogonal test.

* Corresponding author: 15662719116@163.com

The above-mentioned glass-ceramics prepared from blast furnace slag were black or dark gray and had a single color, which made it difficult for these materials to meet individual needs of the current market. It is therefore of interest to develop a process for manufacturing decorative glass-ceramics with attractive colors.

This study used blast furnace water-quenched slag from the Baotou Iron and Steel Group as the main raw material to prepare glass-ceramics. P_2O_5 and CaF_2 were used as nucleating agents. The total mass percentage of the main components (CaO, SiO_2, MgO, and Al_2O_3) of the slag was as high as 88 % – 96 %. In addition, there were small amounts of CaF_2 and TiO_2 in the slag, which can act as crystal nucleating agents, while the presence of K_2O and Na_2O in the slag can lower the melting point of the glass. Therefore, blast furnace slag is an ideal raw material for preparing CaO-SiO_2-MgO-Al_2O_3 series glass-ceramics. The prepared materials are light green and have a luster similar to that of jade. They can be used for interior decorating materials to replace wall tiles, and to make ornaments and jewelry. This product has broad market prospects.

In the preparation of glass-ceramics, the heat treatment process has an important influence on the mechanics and performance of the product, and can improve production efficiency and quality. In this study, an orthogonal experimental design was used to study the influence of the four main process parameters of nucleation and crystallization temperature and time on the flexural strength and microstructure of light-green blast furnace slag glass-ceramics.

II. Experimental Procedure

(1) Preparation of basic glass

The chemical composition of the blast furnace water-quenched slag from the Baotou Iron and Steel Group was analyzed by means of X-ray fluorescence (XRF) [12] and is shown in Table 1. The basic glass composition was selected based on the wollastonite (PDF card 42 – 0550) and pyroxene (PDF card 88 – 0851) region of the quaternary system CaO-Al_2O_3-SiO_2-MgO (Fig. 1) [13]. The chemical components in Table 2 were introduced from the chemical components contained in 50 g blast furnace slag, and SiO_2 was introduced as quartz sand. The remaining chemical components were introduced in the form of pure reagents, totaling about 100 g. The slag contained only small amounts of CaF_2 and TiO_2, so additional amounts of CaF_2 and P_2O_5 (as $Na_3PO_4{\cdot}12H_2O$) were added as composite nucleating agents to form a fluorapatite (PDF card 15 – 0876) [14] crystal phase.

The chemical composition of the basic glass is shown in Table 2.

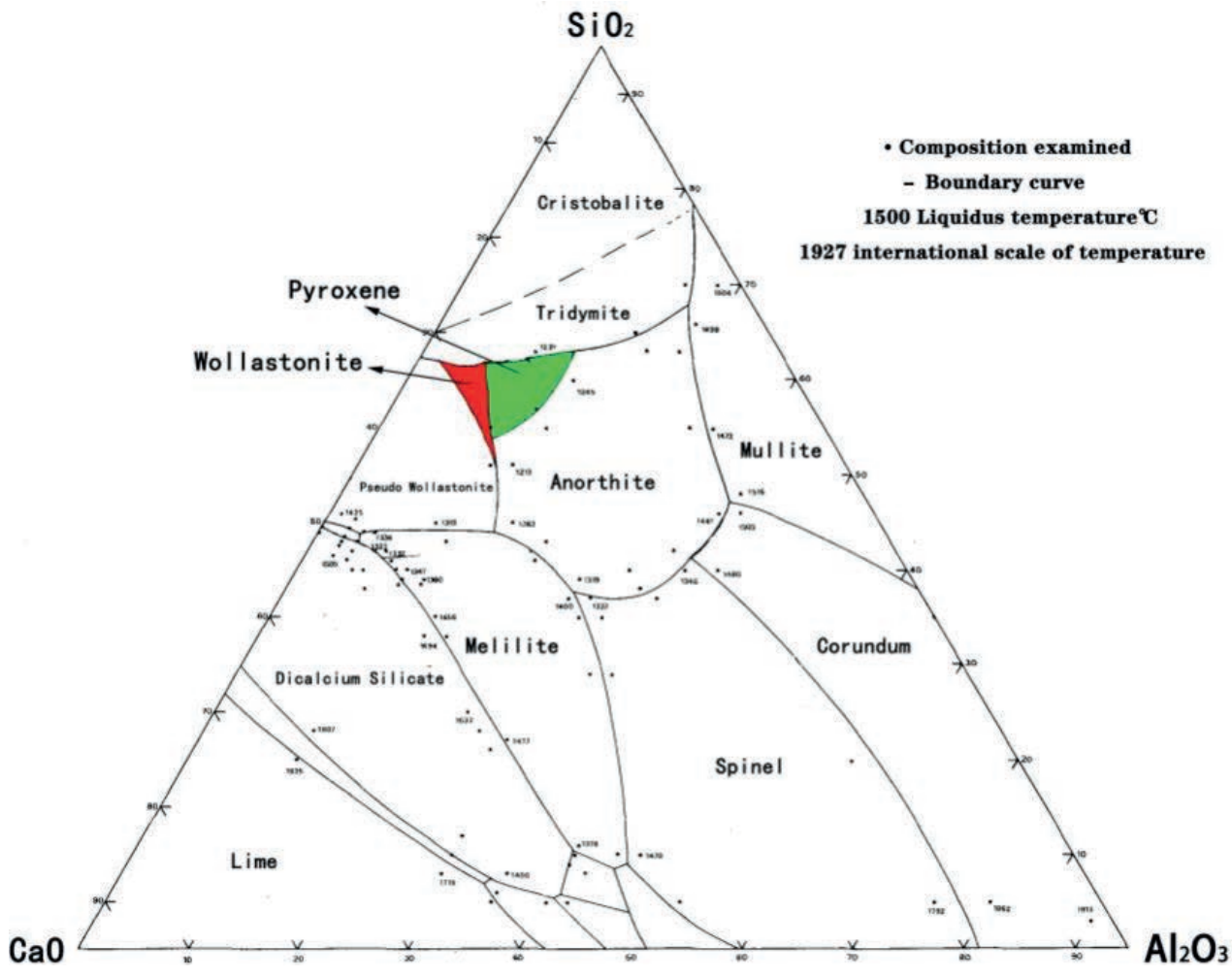

Fig. 1: Liquidus surface of the 5 % magnesia plane in the quaternary system CaO-Al_2O_3-SiO_2-MgO.

Table 1: Chemical composition of blast-furnace slag from the Baotou Iron and Steel Group (mass%)

CaO	SiO_2	Al_2O_3	MgO	CaF_2	CaS	MnO	FeO	K_2O	Na_2O	TiO_2	others
34.9	34.6	14.0	9.3	0.8	3.2	0.5	0.7	0.5	0.5	0.9	0.1

Table 2: Main chemical composition of basic glass (mass%)

SiO_2	CaO	MgO	Al_2O_3	Na_2O	P_2O_5	CaF_2	others
44.7	18.8	4.7	7.0	10.8	8.0	3.0	3.0

The slag was crushed, ground, dried, and passed through a 200-mesh sieve (≤0.074 mm). The raw materials were accurately weighed according to the designed basic glass formula, placed in a clean dry mixing tank, and mixed thoroughly for 3 h. The mixture was placed in a corundum crucible in a high-temperature atmospheric furnace, heated to 1 500 °C, and held for 3 h to melt and clarify the material. The molten glass was cast into a stainless-steel mold that had been preheated to 600 °C. The molten glass was annealed in the mold in a muffle furnace at 600 °C for 2 h to eliminate internal stresses. The basic glass was obtained after cooling in the furnace [15].

(2) Preparation and research method

The prepared basic glass was ground into a powder, and heated from room temperature to 1 200 °C at a heating rate of 10 K/min in an argon atmosphere using an integrated thermal analyzer [16] (STA PT 1600, Linseis, Germany). The nucleation and crystallization temperatures of the glass-ceramics were determined by means of differential scanning calorimetry (DSC) [17].

An X'Pert PRO diffractometer (Philips, Netherlands) was used to perform X-ray diffraction (XRD) analysis on the heat-treated glass-ceramic samples to determine their mineral composition. X-ray diffraction analysis was performed with CuKα radiation. X-ray patterns were captured with the scanning speed of 2°/min under 40 kV and 30 mA working conditions [18].

A field-emission scanning electron microscope (FE-SEM; Sigma 500, Zeiss, Germany) was used to observe the microstructure of the heat-treated samples. Samples were prepared by cutting, grinding, and polishing a section, which was then etched in 5 mass% HF for 30 s, cleaned with distilled water, and coated with gold.

A CSS-88000 electronic universal testing machine was used to evaluate the glass-ceramics with the three-point bending method. The sample size was 4 mm × 4 mm × 40 mm, the range was 30 mm, and the loading speed was 0.5 mm/min [19]. The flexural strength formula is shown in Eq. (1)

$$\sigma = \frac{3FL}{2bh^2}, \qquad (1)$$

where σ is the flexural strength (MPa), F is the maximum load borne by a specimen at fracture (N), b is the fracture width (mm), h is the fracture height (mm), and L is the length of the specimen (mm).

(3) Orthogonal heat treatment design

An orthogonal experimental design was used to optimize the heat treatment process for the basic glass. The flexural strength of the resulting glass-ceramic was used as the assessment index. The nucleation and crystallization temperature ranges of the basic glass were determined from the DSC curve [19] (Fig. 2). There was a slight endothermic peak at 635 °C and an obvious exothermic peak at 822 °C. Glass is an amorphous state with an irregular structure, and its microcrystallization requires stages of both crystal nucleation and growth. Nucleation is the formation of a new phase, which requires a certain amount of energy to establish a surface between the new and parent phases, so the free energy of the system rises and a certain amount of energy needs to be absorbed. Crystallization is the transformation of an unstable glass state to a stable crystalline state that has lower free energy, so energy is released during the crystallization process. The optimal nucleation temperature range of glass-ceramics is generally 50 – 100 °C higher than the glass transition temperature (i.e. the endothermic peak of the DSC curve) and the crystallization temperature is generally the peak temperature of the crystallization exothermic peak [20]. Therefore, based on the DSC curve, a four-factor four-level $L_{16}(4^4)$ orthogonal heat-treatment experimental program was designed, with the factor levels shown in Table 3. The four factors were: nucleation temperature (ranging from 610 to 685 °C, with a step size of 25 °C); nucleation time and crystallization time (both ranging from 1.0 – 2.5 h, with a step

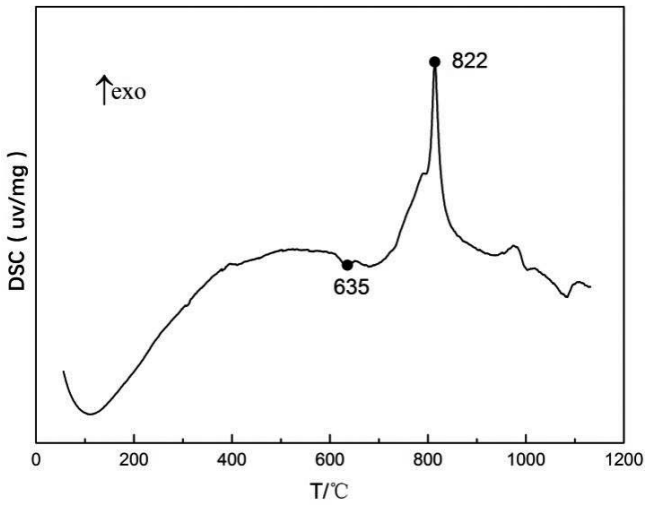

Fig. 2: Differential scanning calorimetry curve of basic glass.

change of 0.5 h); crystallization temperature (ranging from 812 – 842 °C, with a step size of 10 °C).

III. Experimental Results and Analysis

(1) Results of orthogonal experiments

Table 4 lists the orthogonal experimental scheme and results of the flexural strength measurements. Each experimental point was measured three times and the average value reported. Parameters *K*1, *K*2, *K*3, and *K*4 are the average flexural strength values of the first, second, third, and fourth levels of each influencing factor. *R* represents the range, which refers to the difference between the maximum and minimum flexural strengths for each influencing factor at the different levels: the larger the range, the greater the influence of the factor on the flexural strength of the glass-ceramic [21].

Table 3: Levels of test factors

Four factors	Four levels			
	1	2	3	4
Nucleation temperature (°C)	610	635	660	685
Nucleation time (h)	1.0	1.5	2.0	2.5
Crystallization temperature (°C)	812	822	832	842
Crystallization time (h)	1.0	1.5	2.0	2.5

Table 4: Orthogonal heat-treatment process and flexural strength measurements of glass-ceramics

No.	Nucleation temperature/°C	Nucleation time/h	Crystallization temperature/°C	Crystallization time/h	Flexural strength/MPa
1	610	1	812	1	38.73
2	610	2.5	842	2	41.57
3	610	2	832	1.5	16.38
4	610	1.5	822	2.5	41.45
5	635	1.5	812	1.5	25.22
6	635	2.5	832	1	24.21
7	635	2	842	2.5	30.77
8	635	1	822	2	37.16
9	660	2	812	2	29.13
10	660	1.5	842	1	38.19
11	660	1	832	2.5	27.99
12	660	2.5	822	1.5	64.32
13	685	2.5	812	2.5	33.91
14	685	2	822	1	41.44
15	685	1	842	1.5	26.16
16	685	1.5	832	2	48.72
K1	34.53	32.51	31.75	35.64	
K2	29.34	38.40	46.09	33.02	
K3	39.91	29.43	29.33	39.15	
K4	37.56	41.00	34.17	33.53	
*R*1~*R*4	10.57	11.57	16.76	6.13	
Optimal level	660	2.5	822	2	76.83

Table 4 shows that the four factors of nucleation temperature, nucleation time, crystallization temperature, and crystallization time gave the following respective ranges: $R1$ = 10.57, $R2$ = 11.57, $R3$ = 16.76, $R4$ = 6.13. Therefore, the primary and secondary orders of influence on the flexural strength of the glass-ceramics are crystallization temperature > nucleation time > nucleation temperature > crystallization time. In addition, according to the values of $K1$ to $K4$, the best heat treatment system is inferred as a nucleation temperature of 660 °C, a nucleation time of 2.5 h, a crystallization temperature of 822 °C, and a crystallization time of 2 h. Under these heat treatment conditions, the flexural strength of the glass-ceramic reached 76.83 MPa, which is much higher than the flexural strength results of the 16 test points selected by the orthogonal experiments. The glass-ceramics prepared with the optimal heat treatment system were light green and jade-like, as shown in Fig. 3.

Fig. 3: Photograph of glass-ceramic samples.

(2) X-ray diffraction and energy-dispersive spectroscopy results

P_2O_5 was introduced into the basic glass in the form of $Na_3PO_4{\cdot}12H_2O$. The mass percentages of P_2O_5 and Na_2O in the basic glass raw material were 8 % and 10.83 %, respectively, so the basic glass became a multicomponent system of CaO-SiO_2-MgO-Al_2O_3-Na_2O-P_2O_5-CaF_2. To ascertain the devitrifying mineral composition of this system, the 3 and 12 samples, which had the smallest and largest flexural strengths in Table 4, respectively, and the glass-ceramic sample produced under the best heat treatment process conditions were selected for XRD analysis. The results are shown in Fig. 4.

The blast furnace slag accounted for 50 % of the raw material in this study. Except for the introduction of SiO_2 in the form of quartz sand (SiO_2 purity: 98.2 %), the remaining small amounts of CaO, MgO, Al_2O_3, CaF_2, and $Na_3PO_4{\cdot}12H_2O$ were introduced in the form of pure reagents. The waters of crystallization in the pure reagents were removed during the heating process. The glass-ceramics obtained after heat treatment were all light-green jade-like materials. The XRD curves of the three glass-ceramic samples (Fig. 4) show that the precipitated mineral was fluorapatite, $Ca_5(PO_4)F_3$ (PDF card 15 – 0876). There was only a slight difference in diffraction peak intensity between the samples.

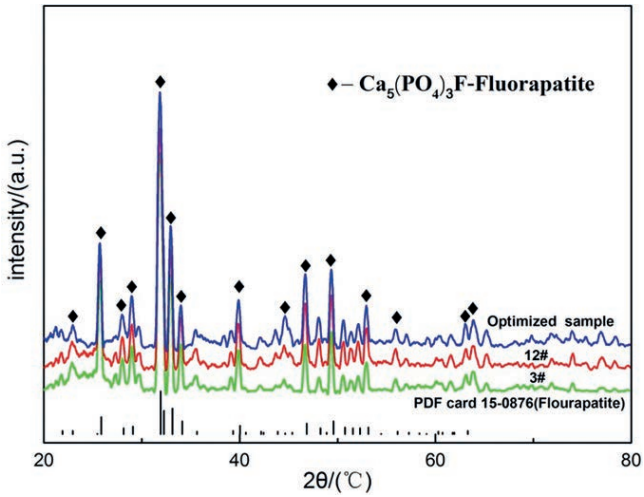

Fig. 4: X-ray diffraction patterns of glass-ceramic samples.

SEM-EDS micro-area analysis was performed on crystal grains in the glass-ceramics, as shown in Fig. 5. O, Ca, Si, F, P, and other elements were enriched in the crystal grains. Si originated from the residual glass phase, while the other elements were consistent with those present in fluorapatite, confirming that this was the main mineral precipitated during heat treatment of the basic glass. The heat treatment had no effect on the composition of the main crystalline phase of the glass-ceramics — only the crystallization rate. P_2O_5 and CaF_2, introduced as a composite nucleating agent, are the main factors that promote the precipitation of fluorapatite $Ca_5(PO_4)F_3$. They not only play the role of nucleating agent in the glass crystallization process, but also participate in the composition of the main crystalline phase. This was the main reason for the crystal phase of the blast furnace slag glass-ceramics prepared in this study differing from those (wollastonite, pyroxene) identified in most other studies.

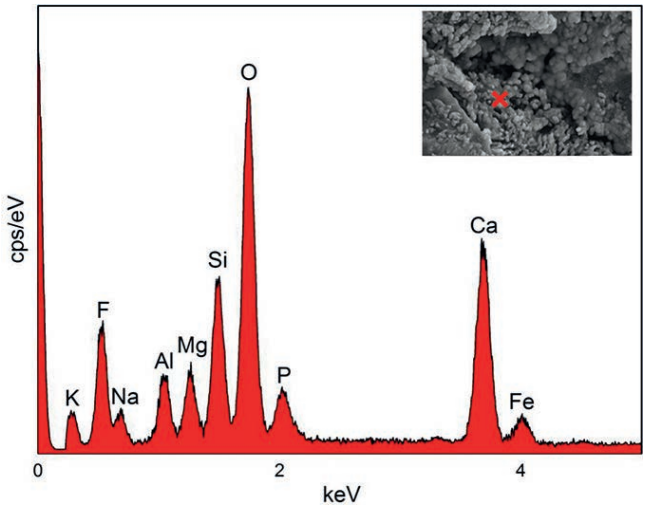

Fig. 5: Energy-dispersive spectrum of crystal particle.

Fluoride is an opacifier for glass. It separates from the glass melt during cooling (or heat treatment), forming fine crystalline precipitates and causing glass turbidity. Using this principle, fluoride can act as a nucleation center to promote the formation of crystal nuclei in the glass [22]. P_2O_5

is a glass-network-forming body that creates an asymmetric phosphoric-acid polyhedron in the silicon-oxygen network. P^{5+} ions have higher field strength and can seize more non-oxygen bridges (free O^{2-}), while F^- and O^{2-}, which have similar radii, can replace O^{2-} and enter the phosphoric-acid polyhedron, thereby facilitating separation of fluorapatite from the glass matrix to form an independent phase [23].

(3) Microstructure analysis

It can be seen from the SEM photo in Fig. 6 that the microstructure of glass-ceramics consists of a crystal phase (A stands for crystalline phase) and a glass phase (B stands for glass phase). An SEM micrograph of the 3 sample (with the smallest flexural strength) (Fig. 6(a)) showed that this contained a large proportion of glass phase, the number of crystal grains was small, and their distribution was uneven. With the orthogonal experiment in Table 4 to obtain the range, it can be established that the crystallization temperature was the main influencing factor that affects the flexural strength of the glass-ceramics. The influence of nucleation temperature was the third factor. *K*3 was 29.43 MPa, which was the smallest average value of the flexural strength among the four crystallization temperatures, indicating that the crystallization temperature of 832 °C was the most unfavorable for the crystallization of glass-ceramics. This was the reason that the flexural strength of 3 sample had low flexural strength (16.38 MPa). For the 12 sample with higher flexural strength (Fig. 6(b)), the proportion of glass phase was greatly reduced, the number of crystal grains was obviously increased, and the integrity of the crystal grains was improved. The flexural strength (64.32 MPa) of this sample was significantly higher. The main reason was that the crystallization temperature was the peak temperature in the DSC curve (822 °C).

The microstructure of the glass-ceramic sample obtained in the optimal heat treatment process is shown in Fig. 6(c). Compared with the 12 sample, the number of crystal grains further increased, and their distribution was more uniform and dense. The main reason is that the crystallization time has been extended to 2.5 h at 822 °C. After heat treatment, the microstructure achieved a more ideal state and the flexural strength was highest, reaching 76.83 MPa. According to related literature [24 – 25], the smaller the crystal grains, the higher is their number, the more uniform is the distribution, and the higher is the resulting strength. When Hall [26] and Petch [27] studied the relationship between the tensile strengths of zinc and steel and their grain sizes, the fracture strength or yield strength and grain size conformed to the following formula (2):

$$\delta_f = \delta_0 + Kd^{-1/2}, \qquad (2)$$

where δ_f is the breaking strength (MPa), δ_0 and K are material constants, and d is the grain diameter (μm). For polycrystalline materials, the grain boundaries are weaker than the inside of the grains, so fracture mainly occurs along grain boundaries. The finer the grains in a material and the greater their number, the longer is the distance that a crack must travel when fracturing along a grain boundary, so the greater the energy that is required and the higher the strength of the material. This is the reason that the glass-ceramic sample prepared with the optimal heat treatment protocol exhibited higher flexural strength than the other samples.

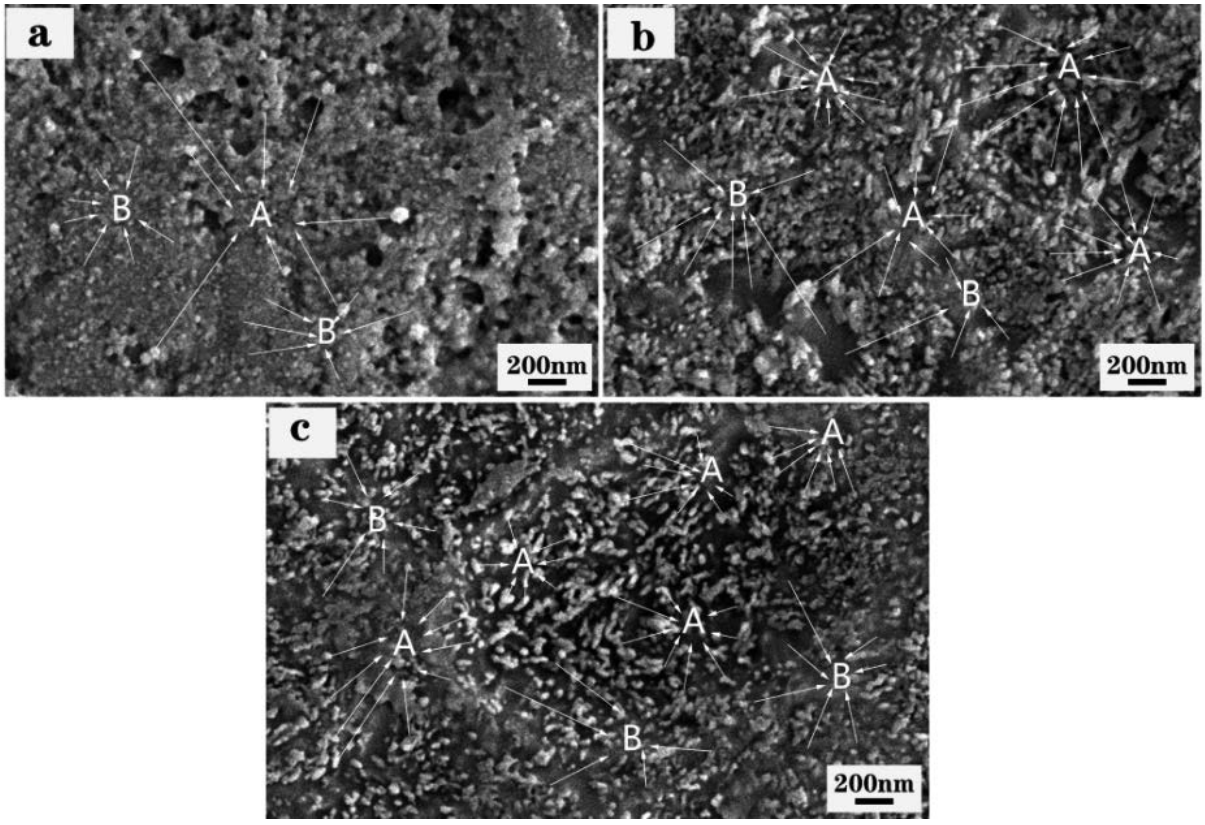

Fig. 6: Scanning electron micrograph of heat-treated glass-ceramics: (a) Sample # 3, (b) Sample # 12, and (c) sample prepared under optimized conditions (A stands for crystalline phase, B stands for glass phase).

IV. Conclusions

(1) A four-factor four-level orthogonal experiment design ($L_{16}(4^4)$) was used to optimize the heat treatment for preparing light-green jade-colored glass-ceramics from the Baotou Iron and Steel Group blast furnace water-quenched slag. The primary and secondary orders that affect the flexural strength of glass-ceramics are the crystallization temperature > nucleation time > nucleation temperature > crystallization time. The optimal heat treatment comprised a nucleation temperature of 660 °C, nucleation time of 2.5 h, crystallization temperature of 822 °C, and crystallization time of 2 h.

(2) XRD and SEM-EDS analysis showed that the main crystal phase of the light-green jade-colored blast furnace slag glass-ceramics was fluorapatite, $Ca_5(PO_4)F_3$. The heat treatment process did not affect the main type of crystal phase.

(3) The light-green jade-colored blast furnace slag glass-ceramic produced with the optimal heat treatment system exhibited flexural strength up to 76.83 MPa. The high degree of crystallinity, large number of crystal grains, and uniform and compact distribution were the main reasons for improvement of the flexural strength of glass-ceramics following process optimization.

Acknowledgements

This work was financially supported by the Joint Project of Inner Mongolia Natural Science Foundation (2018LH05026) and Special Project for Transformation of Scientific and Technological Achievements in Inner Mongolia (2019 CG073) and "Solid Waste Resource" National Key Research & Development Project (2020YFC1909105).

References

1 Reddy, A.A., Eghtesadi, N., Tulyaganov, D.U., Pascual, M.J., Ferreira, J.: Bi-layer glass-ceramic sealant for solid oxide fuel cells, *J. Eur. Ceram. Soc.*, **34**, [5], 1449 – 1455, (2014).

2 Hisham, N., Zaid, M., Saparuddin, D.I., Aziz, S., Iwamoto, Y.: Crystal growth and mechanical properties of porous glass-ceramics derived from waste soda-lime-silica glass and clam shells, *J. Mater. Res.*, **9**, [4], 9295 – 9298, (2020).

3 Rao, A.S., Ashok, J., Suresh, B., Raju, G.N., Venkatramaiah, N., Kumar, V.R., Kityk, I.V., Veeraiah, N.: Physical characteristics of PbO-ZrO_2-SiO_2:TiO_2 glass ceramics embedded with $Pb_2Ti_2O_6$ cubic pyrochlore crystal phase: Part-I electrical properties, *J. Alloy Compd.*, **712**, 672 – 686, (2017).

4 Ovecoglu, M.L.: Microstructural characterization and physical properties of a slag-based glass-ceramic crystallized at 950 and 1100 °C, *Ceram. Int.*, **18**, [2], 391 – 396, (1998).

5 Klemantaski, S., Kerrison, B.: Slag ceramic: A new construction material, *Chem. Ind. (London)*, [10], 1745 – 1749, (1966).

6 Agarwal, G., Speyer, R.F.: Devitrifying cupola slag for use in abrasive products, *JOM.*, **44**, [3], 32 – 37, (1992).

7 Khater, G.A.: The use of saudi slag production of glass-ceramic materials, *Ceram. Int.*, **18**, [1], 59, (2002).

8 Francis, A.A.: Crystallization kinetics of magnetic glass-ceramics prepared by the processing of waste materials, *Mater. Res. Bull.*, **41**, [6], 1146 – 1154, (2006).

9 Fan, C.S, Li, K.C.: Glass-ceramics produced from thin-film transistor liquid-crystal display waste glass and blast oxygen furnace slag, *Ceram. Int.*, **40**, [5], 7117 – 7123, (2014).

10 Zhang, Z., Wang, H., Shan, Q., Ma, L., He, P.: Experimental study on the direct preparation of glass-ceramic from the slag of blast-furnace, *Proc. Int. Conf. Power Eng. (ICOPE)*, (2009).

11 Zhao, Y., Chen, D.F., Bi, Y.Y., Long, M.J.: Preparation of low-cost glass-ceramics from molten blast furnace slag, *Ceram. Int.*, **38**, [3], 2495 – 2500, (2012).

12 Gregory, B., Patterson, R.T., Reinhardt, E.G., Galloway, J.M., Roe, H.M.: An evaluation of methodologies for calibrating itrax X-ray fluorescence counts with ICP-MS concentration data for discrete sediment samples, *Chem. Geol.*, **521**, 12 – 27, (2019).

13 Vázquez, B.A., Caballero, A., Pena, P.: Quaternary system Al_2O_3-CaO-MgO-SiO_2: I, study of the crystallization volume of Al_2O_3, *J. Am. Ceram. Soc.*, **86**, [12], 2195 – 2199, (2010).

14 Zahrani, E.M., Fathi, M.H., Alfantazi, A.M.: Sol-gel derived nanocrystalline fluoridated hydroxyapatite powders and nanostructured coatings for tissue engineering applications, *Metall. Mater. Trans. A*, **42**, [11], 3291 – 3309, (2010).

15 Babkina, A.N., Zyryanova, K.S., Agafonova, D.A., Nuryev, R.K., Valiev, D.: The effect of chromium concentration on luminescent properties of alkali-alumina-borate glass-ceramics, *J. Non-Cryst. Solids*, **521**, 119487, (2019).

16 Li, B.W., Li, H.X., Zhang, X.F., Jia, X.L., Sun, Z.C.: Nucleation and crystallization of tailing-based glass-ceramics by microwave heating, *Int. J. Miner. Metall. Mater.*, (22), 1349 – 1349, (2015).

17 Tunali, A., Ozel, E., Turan, S.: Production and characterisation of granulated frit to achieve anorthite based glass-ceramic glaze, *J. Eur. Ceram. Soc.*, **35**, 1089 – 1095, (2015).

18 Huang, Y., Zhao, B., Fang, J., Ran, A., Sun, Y.: Tunning of microstructure and thermoelectric properties of $Ca_3Co_4O_9$ ceramics by high-magnetic-field sintering, *J. Appl. Phys.*, **110**, [12], 134423, (2011).

19 Yang, J., Zhang, S.G., Liu, B., Pan, D.A., Chun-Li, W.U., Avolinsky, A.: Effect of TiO_2 on crystallization, microstructure and mechanical properties of glass-ceramics, *J. Iron. Steel Res. Int.*, **22**, (012), 1113 – 1117, (2015).

20 Gorelik, V.S., Golovina, T.G., Konstantinova, A.F.: Central peak in the raman spectra of quartz crystals in a wide temperature range, *Crystallogr. Rep.*, **65**, [4], 605 – 611, (2020).

21 Peng, F., Liang, K.M., Hu, A.M.: Nano-crystal glass-ceramics obtained from high alumina coal fly ash, *Fuel*, **84**, [4], 341 – 346, (2005).

22 Kim, S.T., Park, H.J., Yoon, M.Y., *et al.*: Effect of heat treatment on the cellulose-calcium silicate nanocomposites synthesis from waste wood, clam shell, and glass, *Adv. Appl. Ceram.*, **113**, [6], 346 – 351, (2014).

23 Nascimento, M.L.F.: Centenary of a serendipitous Inventor: stookey and a short statistical overview of photosensitive glass & glass-ceramics science and technology, *Recent Pat. Mater. Sci.*, **9**, [1], (2016).

24 Sasaki, T., Yanase, A., Dai, O., Kariya, Y., Ikeda, T.: Measurements and FEM analyses of strain distribution in small sn specimens with few crystal grains, *Mater. Trans.*, JIM, **60**, [6], (2019).

25 Nazari, A., Riahi, S.: The effects of ZnO_2 nanoparticles on strength assessments and water permeability of concrete in different curing media, *Mater. Res.*, **14**, [2], (2011).

26 Hall, E.O.: The deformation and ageing of mild steel: II characteristics of the Lüders deformation, Proc. Phys. Soc. B, **64**, [9], 742, (1951).

27 Petch, N.J.: The cleavage strength of polycrystals, *J. Iron Steel Inst.*, **174**, 25 – 28, (1953).